Short-term high-fat feeding exacerbates degeneration in retinitis pigmentosa by promoting retinal oxidative stress and inflammation

Oksana Kutsyr[a], Agustina Noailles[a], Natalia Martínez-Gil[a], Lucía Maestre-Carballa[a], Manuel Martinez-Garcia[a], Victoria Maneu[b], Nicolás Cuenca[a,c,1], and Pedro Lax[a,1]

[a]Department of Physiology, Genetics and Microbiology, University of Alicante, 03690 Alicante, Spain; [b]Department of Optics, Pharmacology and Anatomy, University of Alicante, 03690 Alicante, Spain; and [c]Institute Ramón Margalef, University of Alicante, 03690 Alicante, Spain

A high-fat diet (HFD) can induce hyperglycemia and metabolic syndromes that, in turn, can trigger visual impairment. To evaluate the acute effects of HFD feeding on retinal degeneration, we assessed retinal function and morphology, inflammatory state, oxidative stress, and gut microbiome in dystrophic retinal degeneration 10 (rd10) mice, a model of retinitis pigmentosa, fed an HFD for 2 to 3 wk. Short-term HFD feeding impaired retinal responsiveness and visual acuity and enhanced photoreceptor degeneration, microglial cell activation, and Müller cell gliosis. HFD consumption also triggered the expression of inflammatory and oxidative markers in rd10 retinas. Finally, an HFD caused gut microbiome dysbiosis, increasing the abundance of potentially proinflammatory bacteria. Thus, HFD feeding drives the pathological processes of retinal degeneration by promoting oxidative stress and activating inflammatory-related pathways. Our findings suggest that consumption of an HFD could accelerate the progression of the disease in patients with retinal degenerative disorders.

retinal degeneration | neurodegeneration | cell death | gut microbiome

Obesity and diabetes have reached epidemic proportions worldwide (1). It is widely accepted that a high-fat diet (HFD) can induce metabolic dysfunction, which is associated with an increased risk of obesity, metabolic syndrome, and other health complications (2). Accordingly, high-fat feeding is a model of insulin resistance and type 2 diabetes mellitus (3). In this context, it has been demonstrated that acute high-fat feeding (3 to 4 d) in mice increases blood glucose and insulin levels and impairs glucose tolerance and insulin sensitivity (4). Moreover, it has been reported that short-term HFD induces adipose tissue inflammation (4, 5), which contributes to hepatic insulin resistance (4). High-fat intake has also been linked to microbiota dysbiosis through several mechanisms such as increasing gut permeability and inflammation, in turn, influencing the development of such diseases as cancer, cardiovascular diseases, diabetes, and central nervous system disorders (6, 7). In the central nervous system, a number of metabolic disorders associated with HFD, including hyperglycemia, insulin resistance, dyslipidemia, and hypertension, are known risk factors for cognitive dysfunction (8, 9), and it has been demonstrated that a high intake of saturated fats exacerbates neurodegeneration in animal models of dementia, including Alzheimer's (10) and Parkinson's (11) diseases.

In the retina, HFD-induced metabolic alterations impact cell homeostasis and influence retinal function and health (12, 13). It has been reported that HFD-induced prediabetes/early diabetes has a detrimental effect on retinal neuronal activity (13) and triggers retinal inflammation and microvascular dysfunction (14, 15). Moreover, metabolic syndrome is a proven risk factor for the development of diabetic retinopathy (16) and age-related macular degeneration (17), and a positive association between total fat intake and incidence of this disease has been demonstrated (18, 19). Furthermore, HFD-induced gut dysbiosis has been reported to influence retinal degeneration (20).

The above studies support the hypothesis that increased fat intake might affect cellular responses following retinal injury or during degenerative diseases, even after short periods of time. Against this background, we sought to assess the effects of 2 or 3 wk of HFD on the retina of retinal degeneration 10 (rd10) mice, an animal model of retinitis pigmentosa (RP). We found that short-term high-fat feeding drives degenerative changes in the retina of rd10 mice at the molecular, histological, and functional level. Overall, our findings indicate that diets high in fat accelerate the pathologic processes in retinal degenerative diseases, even if consumed for a short time.

Results

Short-Term HFD Promotes Weight Gain and Reversible Glucose Intolerance. No differences were observed for body weight among the experimental groups at the time of weaning, but the introduction of an HFD led to more weight gain than the normal chow diet independently of the mouse genotype and diet period (Fig. 1*A* and *SI Appendix*, Table S1). As expected, males gained more weight than females, with significant differences in almost all experimental groups (*SI Appendix*, Table S1). No differences were found in body weight between control

NEUROSCIENCE

Fig. 1. Metabolic parameters and retinal function are affected by high-fat feeding. (*A*) Body weight in control C57BL/6J and dystrophic rd10 mice after 0, 2, or 3 wk of normal or HFD from postnatal day 19 (n = 7 to 55). (*B* and *C*) Plasma glucose concentrations 0, 30, 60, 90, and 120 min after intraperitoneal injection of glucose (2 g/kg body weight) in fasted C57BL/6J and rd10 mice following 2 (*B*) or 3 (*C*) wk of dietary treatment (n = 7 to 15). (*D*) Glucose tolerance tests in rd10 mice 2 wk after the end of a dietary treatment of 2 or 3 wk (n = 4 in all cases). (*E–H*) Representative scotopic ERG responses to 1 log cd s/m^2 flashes (*E* and *G*) and luminance-response curves for the a- and b-waves (*F* and *H*) from C57BL/6J and rd10 mice fed a normal or HFD for 2 (*E* and *F*) or 3 (*G* and *H*) wk (n = 6 to 18). (*I*) Illustration of the optomotor apparatus used in this study (image created using BioRender; https://biorender.com/). (*J* and *K*) Visual acuity measured as the spatial frequency threshold in C57BL/6J and rd10 mice fed a normal or HFD for 2 (*J*) or 3 (*K*) wk (n = 3 to 11). ANOVA, Bonferroni's test, diet effects (normal versus HFD), *$P < 0.05$, **$P < 0.01$, ***$P < 0.001$, ****$P < 0.0001$; ANOVA, Bonferroni's test, strain effects (C57BL/6J versus rd10), ##$P < 0.01$, ###$P < 0.001$.

Kutsyr et al.
Short-term high-fat feeding exacerbates degeneration in retinitis pigmentosa
by promoting retinal oxidative stress and inflammation

(C57BL/6J) mice and dystrophic rd10 mice fed the same diet (Fig. 1*A* and *SI Appendix*, Table S1).

No changes in glycemia were found between control and rd10 mice at the introduction of the diet; however, fasting blood glucose levels in both groups of mice were higher on the HFD than on the chow diet, which became significant after 2 wk on diet (Fig. 1*B* and *SI Appendix*, Table S2). No within-group differences in glycemia were found between males and females. Glucose tolerance was impaired in both control and rd10 mice on the HFD for 2 and 3 wk with respect to the chow diet as shown by the significantly greater blood glucose concentration after a single intraperitoneal injection of D-glucose (2 g/kg body weight) (Fig. 1 *B* and *C*, respectively, and *SI Appendix*, Table S2). Glucose tolerance impairment induced by HFD was more severe in rd10 mice than in control mice irrespective of the dietary period (Fig. 1 *B* and *C* and *SI Appendix*, Table S2). No sex effects were found, with the exception of mice fed with the HFD for 3 wk. To assess the potential for recovery of impaired glucose tolerance, the glucose tolerance test was repeated in a subset of rd10 mice 2 wk after the period of normal or HFD consumption. Results showed no differences in blood glucose levels independently of the diet consumed during the experimental period (Fig. 1*D*).

Short-Term HFD Impairs Retinal Responsiveness in RP Mice. To evaluate the effect of a short-term HFD on the functioning of normal and diseased retinas, we recorded scotopic flash-induced electroretinographic (ERG) responses in control and rd10 animals fed an HFD or chow diet. ERG flash responses were greater in control mice than in rd10 mice irrespective of diet or experimental period, and no diet-related differences were observed in control animals (Fig. 1 *E–H*). An analysis of ERG amplitudes in rd10 mice revealed significant diet-dependent differences, being smaller in high-fat–fed than in the normal-fed animals, independently of the diet period. The maximum amplitudes observed for scotopic a- and b-waves in HFD-fed animals were 48 and 62%, respectively, of the values obtained on the chow diet after 2 wk (Fig. 1*F*). After 3 wk of HFD, the maximum amplitudes for a- and b-waves were 51 and 56%, respectively, of those measured in chow-fed animals (Fig. 1*H*). No sex effects were found.

We next assessed visual acuity using the optomotor test (Fig. 1*I*). Visual acuity thresholds were higher in control mice than in rd10 mice irrespective of the diet and the diet period, and no diet-related differences were observed in control mice (Fig. 1 *J* and *K*). By contrast, visual acuity was significantly lower in rd10 mice fed the HFD than in counterparts on the chow diet irrespective of the diet period (67% after 2 wk on the HFD and 70% after 3 wk) (Fig. 1 *J* and *K*). Overall, these findings indicate that HFD feeding diminishes retinal responsiveness in RP mice.

Short-Term HFD Aggravates Photoreceptor Degeneration in RP Mice. We next examined the effects of short-term HFD on photoreceptor number and morphology. We first quantified the number of photoreceptor rows in retina cross-sections from the different groups after 2 wk of diet. Because the rate of retinal degeneration is not uniform throughout the retina, we calculated the number of photoreceptor rows from the temporal to the nasal side of the retina through the optic nerve head (Fig. 2*A*). The mean number of photoreceptor rows in each of the areas analyzed was considerably greater in control mice than in rd10 mice irrespective of the diet (Fig. 2*B*), and no diet-related differences were found for control mice (Fig. 2*B*). Contrastingly, the mean number of photoreceptor rows in all retinal areas examined in rd10 mice was higher on the chow diet than on the HFD, with significant differences in most of the temporal and nasal areas tested (Fig. 2*B*). On average, the mean

number of photoreceptor rows in rd10 mice on the HFD was 68% of that on the chow diet (2.4 ± 0.3 versus 3.6 ± 0.3 rows).

To evaluate whether short-term HFD consumption affects the morphology of photoreceptors in control and RP mice, we immunolabeled retina cross-sections with antibodies against cone arrestin, a cone-specific marker (21), and rhodopsin (specific for rods) in mice on the different diets for 2 wk. No diet-related differences in retinal morphology were observed in control mice (Fig. 2 *C* and *D*). An analysis of cone morphology in HFD-fed rd10 mice revealed evident degeneration (Fig. 2*F*), and cones were smaller in size with an almost absence of inner and outer segments. In addition, cone axons were nearly lost, and pedicles came out from the cell bodies. In sharp contrast to the findings in HFD-fed rd10 mice, cone photoreceptors in rd10 mice on the chow diet had a more normal morphology (Fig. 2*E*), with a typical cone shape, still visible inner and outer segments, and long axons and normal pedicles, similar to that observed in control mice (Fig. 2*C*). An analysis of rod structures revealed evident deterioration in HFD-fed rd10 mice as compared with chow-fed counterparts (Fig. 2 *E and F*), with shorter rod outer segments (Fig. 2 *E* and *F*). Indeed, rhodopsin immunoreactivity in HFD-fed rd10 mice appeared to be located not only in the outer segments but also in the cytoplasm (Fig. 2*F*, arrowheads). Similar results were obtained in retina cross-sections along the superior–inferior plane (*SI Appendix*, Fig. S1), supporting the findings in the nasal–temporal cross-sections.

Short-Term HFD Reduces Photoreceptor Connectivity in RP Mice. Given the significantly lower number of photoreceptor rows in HFD-fed rd10 mice, we next assessed synaptic connectivity between photoreceptors and secondary neurons in the retina in mice fed chow or HFD for 2 wk. We immunolabeled nasal–temporal retina cross-sections with antibodies against 1) vesicular glutamate transporter type 1 (VGluT1), 2) the alpha isoform of protein kinase C (PKC-α), 3) calbindin, and 4) Bassoon. VGluT1 labels photoreceptor synaptic vesicles in cone and rod axon terminals (22), PKC-α labels ON-rod bipolar cells (23), anti-calbindin antibodies localize horizontal cells (24), and Bassoon marks the synaptic ribbons in both the rod spherules and cone pedicles of the outer plexiform layer (25).

The immunolabeling of rod bipolar cells from control retinas with PKC-α revealed numerous dendrites projecting from labeled cells within the outer plexiform layer (OPL) through large dendritic arbors (Fig. 3*A*, arrowheads), independently of the diet consumed. In the retina of rd10 mice fed normal chow, rod bipolar cells exhibited a relative retraction of their dendrites (Fig. 3*B*, arrowheads), with a smaller number of dendritic branches than those of the control mice. By contrast, bipolar cell dendrites were very scarce in HFD-fed rd10 mice (Fig. 3*C*, arrowheads), and some cells had almost no dendrites.

Calbindin staining in retinas of control mice revealed a punctate staining pattern along the dendrites and axons protruding from horizontal cell bodies, extending their processes into the OPL (Fig. 3*D*, arrowheads). The density and structure of dendritic and axonal arborizations of horizontal cells was comparable in retinas from control mice fed chow or HFD. We observed a relative retraction and loss of horizontal cell neurites in chow-fed rd10 mice as compared with control animals (Fig. 3*E*, arrowheads). By contrast, HFD-fed rd10 mice showed a marked reduction in the dendritic and axonal arborization of horizontal cells, with only a few dendrites evident (Fig. 3*F*, arrowheads).

The staining of photoreceptor synaptic vesicles with VGluT1 revealed a dense strip of labeled photoreceptor terminals in the OPL of control mice, independently of the diet consumed (Fig. 3*D*). The staining for VGluT1 was less evident in chow-fed rd10 mice, although a continuous strip of photoreceptor axon

NEUROSCIENCE
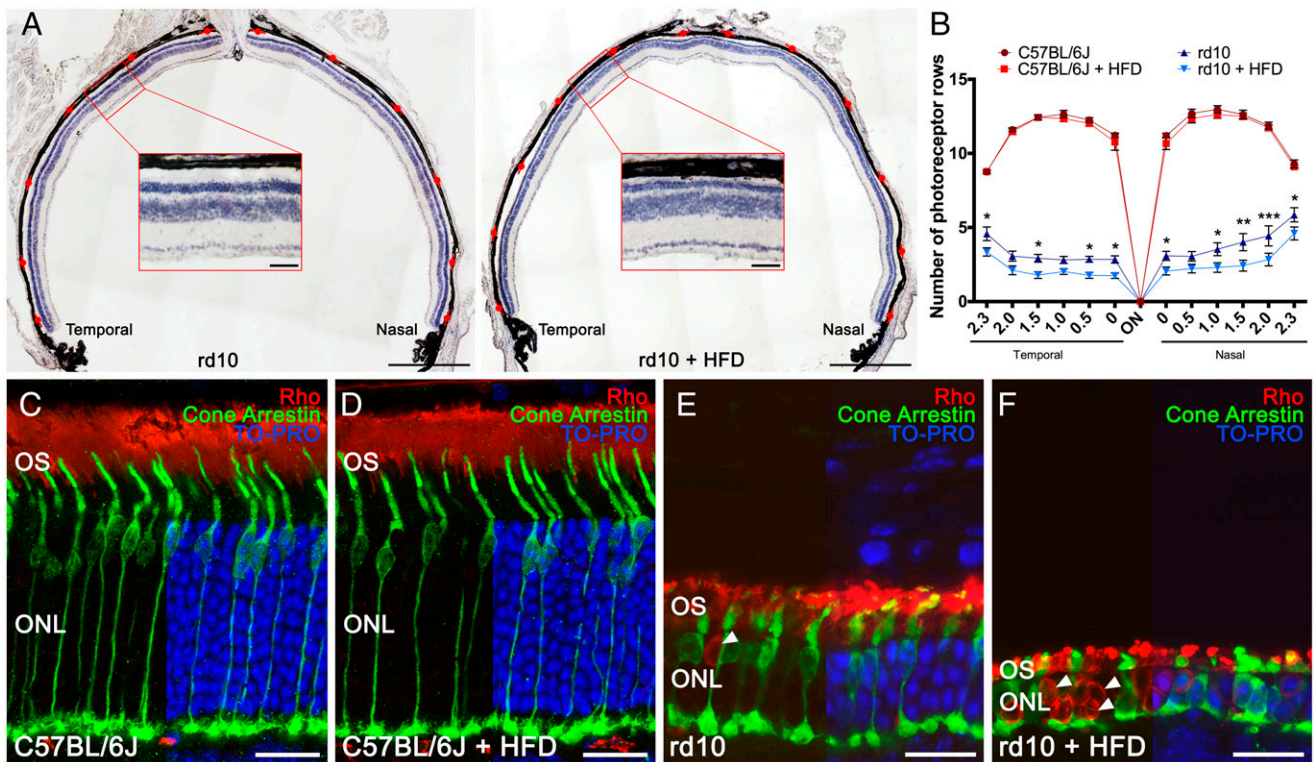
Fig. 2. High-fat intake accelerates photoreceptor cell degeneration. (*A*) Representative nasal–temporal retina cross-sections and high magnification views from rd10 mice fed a normal or HFD for 2 wk from postnatal day 19 stained with hematoxylin. Red marks point to regions where the number of photoreceptor rows was quantified. (*B*) Average number of photoreceptor rows throughout the nasal–temporal axis in C57BL/6J and rd10 mice fed normal or HFD ($n = 3$ for C57BL/6J mice and $n = 8$ to 9 for rd10 mice). (*C–F*) Representative retina cross-sections from C57BL/6J and rd10 mice fed normal chow or HFD immunolabeled against rhodopsin (Rho, rod cells, in red) and cone arrestin (cone cells, in green). TO-PRO 3– (in blue) stained nuclei. In C57BL/6J mice, images show a normal cone photoreceptor morphology and rhodopsin distribution (*C* and *D*), independently of the diet. In rd10 mice, images show morphological alteration of the cones and abnormal distribution of rhodopsin (*E*), both aggravated by HFD consumption (*F*). Arrowheads point to the mislocalization of rhodopsin into the cell bodies (*E* and *F*). ANOVA, Bonferroni's test, diet effects (normal versus HFD), *$P < 0.05$, **$P < 0.01$, ***$P < 0.001$. OS: outer segment. (Scale bars: *A*, 500 μm; Insets, 50 μm; *C–F*, 20 μm.)

terminals could still be observed, indicating the presence of functional photoreceptor synapses (Fig. 3*E*). By contrast, VGluT1 staining was sparse in HFD-fed rd10 mice with few functional photoreceptor axon terminals (Fig. 3*F*), indicating greater degeneration of the axon terminals and resulting in a discontinuous plexus in the OPL. Triple labeling for VGlut1, PKC-α, and calbindin revealed reduced pairings between photoreceptor axons and second-order neuron processes in chow-fed rd10 mice (Fig. 3*G*, arrows). As expected, synaptic contacts between photoreceptor terminals and horizontal cell processes were very scarce in HFD-fed rd10 mice (Fig. 3*H*, arrows). Taken together, our data point to a degenerating effect of short-term HFD consumption on synaptic contacts between photoreceptors and second-order retinal neurons, namely bipolar and horizontal cells. Similar results were obtained in cross-sections along the superior–inferior plane of the retina (*SI Appendix*, Fig. S1), confirming these results.

To quantify the synaptic connectivity between photoreceptors and second-order neurons, we stained retinas with an antibody against Bassoon, a specific component of synaptic ribbons in rod spherules and cone pedicles. Control retinas showed a relatively high density of immunoreactive puncta across the OPL (Fig. 3 *I* and *J*), independently of the diet. Few Bassoon-positive spots were apparent in the retina of chow-fed rd10 mice (Fig. 3*K*) as compared with normal control retinas, and they were even more rare in HFD-fed rd10 mice (Fig. 3*L*). The quantification of Bassoon immunoreactivity at the OPL revealed no significant differences between control mice on the

different diets (Fig. 3*M*). However, Bassoon fluorescence in the OPL was significantly lower in HFD-fed rd10 mice than in chow diet-fed rd10 mice (Fig. 3*M*).

Short-Term HFD Exacerbates Retinal Inflammation in RP Mice. Retinal neurodegeneration is characterized by inflammation that persists along the course of the disease. To assess the effects of short-term HFD feeding on retinal microglia activation, we immunolabeled retina cross-sections from control and rd10 mice fed chow or HFD for 2 wk with antibodies against Iba1, a marker of microglia (26). Analyses of control mice revealed that Iba1+ cells were scarce overall and barely present in the outer retina, showing a morphology with a small soma and numerous thin branching processes, which are typical morphological features of resting microglia (Fig. 4*A*). No diet effects were found in the number or features of retinal Iba1+ cells in control mice (Fig. 4*B*). Iba1+ cells were more abundant in the retina of rd10 mice, with a higher number of Iba1+ cells in chow-fed rd10 mouse retinas than in equivalent control retinas, including abundant Iba1+ cells in the outer nuclear layer (ONL) of these animals (Fig. 4*C*). Furthermore, the somas of Iba1+ cells in rd10 retinas were larger, with shorter and thick processes, a phenotype characteristic of reactive microglia. A comparative analysis of retinas from chow- and HFD-fed rd10 mice revealed a significant increase and a profound migration of microglial cells in the latter (Fig. 4 *D* and *I*), including an increase in the density of these cells in the ONL and in the sub-retinal space (Fig. 4*D*). These results indicate that short-term
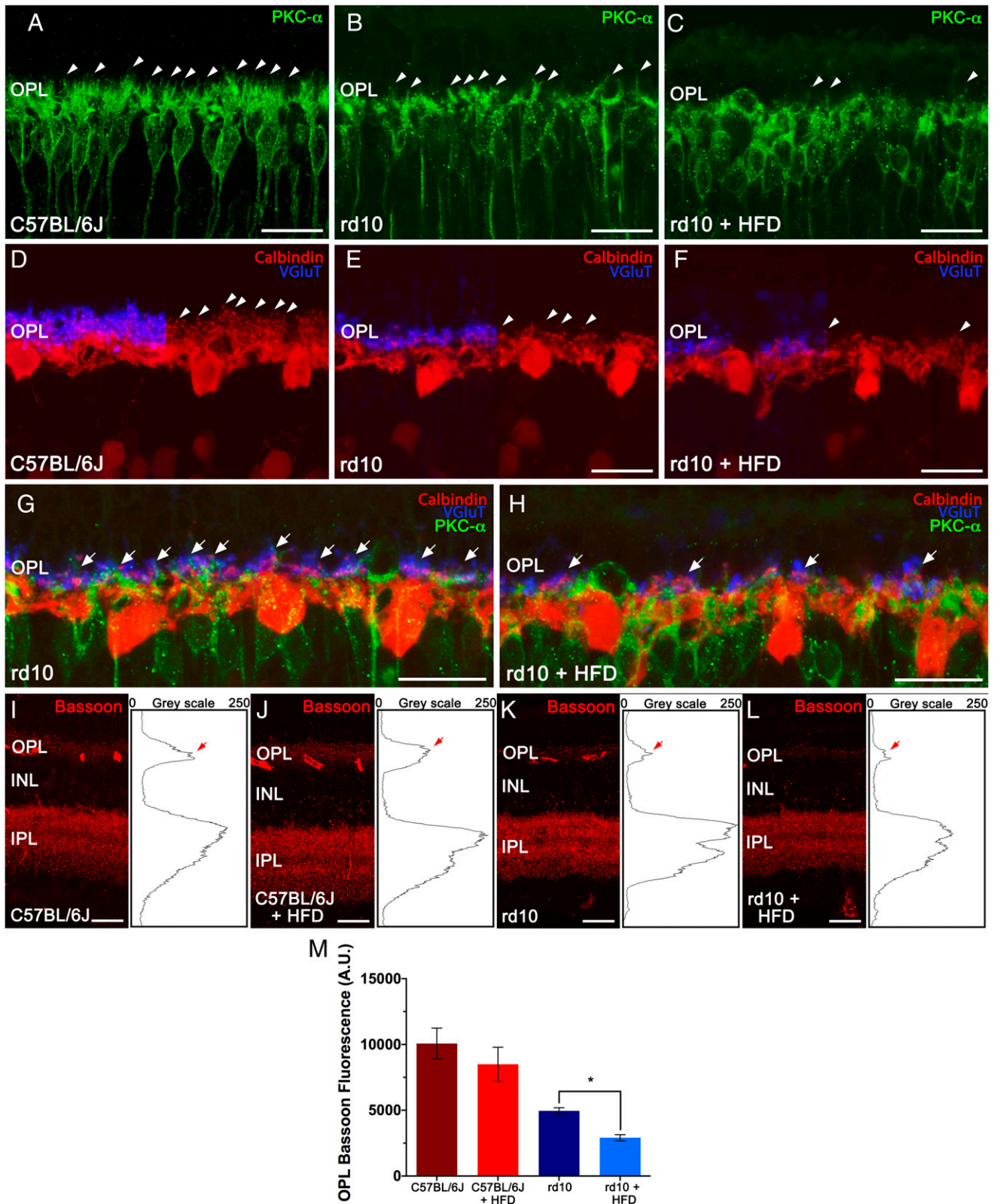
Fig. 3. High-fat consumption alters photoreceptor connectivity and second-order neurons in rd10 mice. (*A–H*) Representative nasal–temporal retina cross-sections from a C57BL/6J mouse fed normal chow and rd10 mice fed a normal or HFD for 2 wk from postnatal day 19 immunolabeled against PKC-α (rod bipolar cells, in green), calbindin (horizontal cells, in red), and VGluT (axon terminals, in blue). Note that dendrites in second-order neurons (arrowheads) and synaptic contacts with photoreceptors (arrows) are more deteriorated after HFD feeding. (*I–L*) Representative retina cross-sections showing synaptic ribbons immunostained with an anti-Bassoon antibody (in red) from C57BL/6J mice fed normal chow (*I*) or HFD (*J*) and rd10 mice fed normal chow (*K*) or HFD (*L*). (*Insets, Right*) The profile plots of mean gray intensity for each horizontal line. (*M*) Quantification of the differential expression of Bassoon in the OPL (arrows in *I–L*). Mann–Whitney *U* test, $n = 4$, *$P < 0.05$. INL: inner nuclear layer, IPL: inner plexiform layer. (Scale bars: 20 μm.)

NEUROSCIENCE
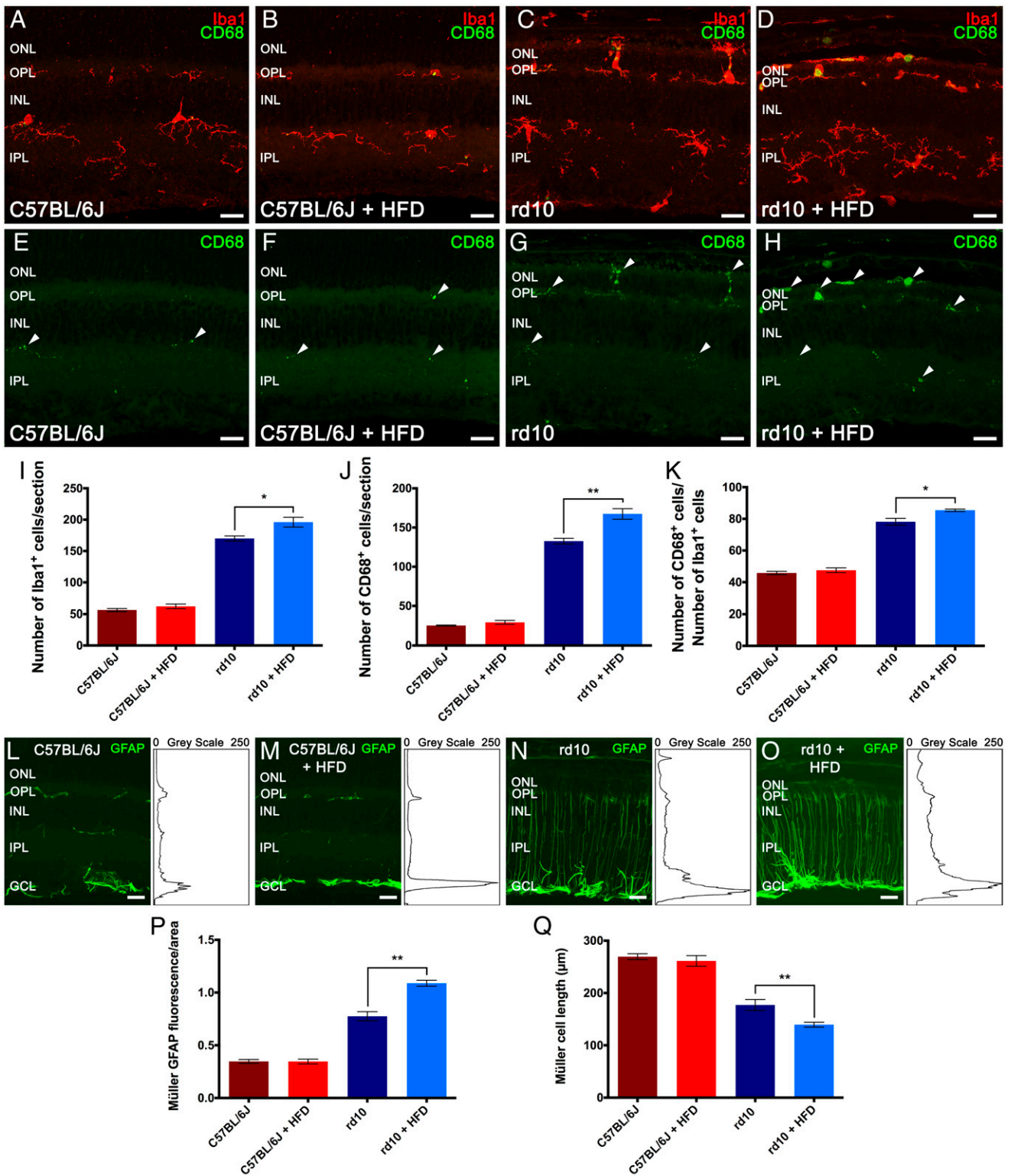
Fig. 4. High-fat feeding activates retinal glial cells. (*A*–*D*) Representative nasal–temporal retina cross-sections from C57BL/6J mice fed normal chow (*A*) or an HFD (*B*) and rd10 mice fed a normal (*C*) or HFD (*D*) for 2 wk from postnatal day 19 immunolabeled against Iba1 (microglia, in red) and CD68 (phagocytic cells, in green). (*E*–*H*) Retina cross-sections of *A*–*D* showing CD68 labeling. Arrowheads point to CD68^{+} microglial cells. (*I*–*K*) Average number of Iba1^{+} (*I*) and CD68^{+} cells (*J*) per retina section and percentage of Iba1^{+} cells labeled for CD68 (*K*). (*L*–*O*) Retina sections of *A*–*D* showing cells immunolabeled for GFAP (activated macroglia, in green). (*Insets*, *Right*) The profile plots of mean gray intensity for each horizontal line. (*P*) Quantification of the differential expression of GFAP. (*Q*) Average length of Müller cells. Images were collected from the central area of the retina, close to the optic nerve. Mann–Whitney *U* test, *n* = 4 for C57BL/6J mice and *n* = 6 for rd10 mice, *$P < 0.05$, **$P < 0.01$. INL: inner nuclear layer, IPL: inner plexiform layer, GCL: ganglion cell layer. (Scale bars: 20 μm.)

Kutsyr et al.
Short-term high-fat feeding exacerbates degeneration in retinitis pigmentosa
by promoting retinal oxidative stress and inflammation

exposure to an HFD provokes changes in Iba1+ cell number and localization throughout the retina of rd10 mice.

To analyze the activation degree of microglial cells, we coimmunolabeled retina cross-sections with antibodies against Iba1 and CD68, a protein expressed on the lysosomal membrane of phagocytic cells and a marker for phagocytic amoeboid microglia (27). In control mice, CD68 positivity was rarely found in the soma of the few Iba1+ cells, independently of the diet consumed (Fig. 4 *E* and *F*, arrowheads). CD68 staining was more robust in rd10 mice fed normal chow (Fig. 4*G*), with a higher density of CD68+ cells (Fig. 4*J*) and a consequent increase in the proportion of cells double positive for Iba1 and CD68 (Fig. 4*K*). Both the density and the percentage of CD68+ cells were significantly augmented in HFD-fed rd10 mice with respect to chow-fed counterparts (Fig. 4 *D*, *H*, *J*, and *K*).

We next assessed the reactive gliosis of astrocytes and Müller cells in retina cross-sections by analyzing the immunoreactivity for glial fibrillary acidic protein (GFAP). No diet effects were found in GFAP immunoreactivity in control retinas, and immunoreactivity was present only in the inner margin of the retina where astrocytes are located (Fig. 4 *L* and *M*). Retinal GFAP immunoreactivity was stronger in rd10 mice than in control mice, both in the inner margin of the retina and also throughout Müller cells (Fig. 4*N*), and was stronger still in the retinas of HFD-fed rd10 mice (Fig. 4*O*) throughout the entire Müller cell length and in the outer retinal areas. These results indicate that short-term feeding of HFD exacerbates reactive gliosis in the rd10 mouse retina.

We quantified the degree of activation of astrocytes and Müller cells by measuring the fluorescence area associated with the GFAP immunostaining and the length of the Müller cells in the retinal sections. No diet-induced differences were found in control mice (Fig. 4 *P* and *Q*), but GFAP immunoreactivity was markedly higher in rd10 mice than in control animals (Fig. 4*P*). Reactive gliosis was significantly higher in the retina of HFD-fed rd10 mice than in chow-fed counterparts (Fig. 4*P*). Furthermore, Müller cell length was significantly shorter in HFD-fed rd10 mice than in chow-fed rd10 mice (Fig. 4*Q*), in agreement with the reduction in retinal thickness in these animals.
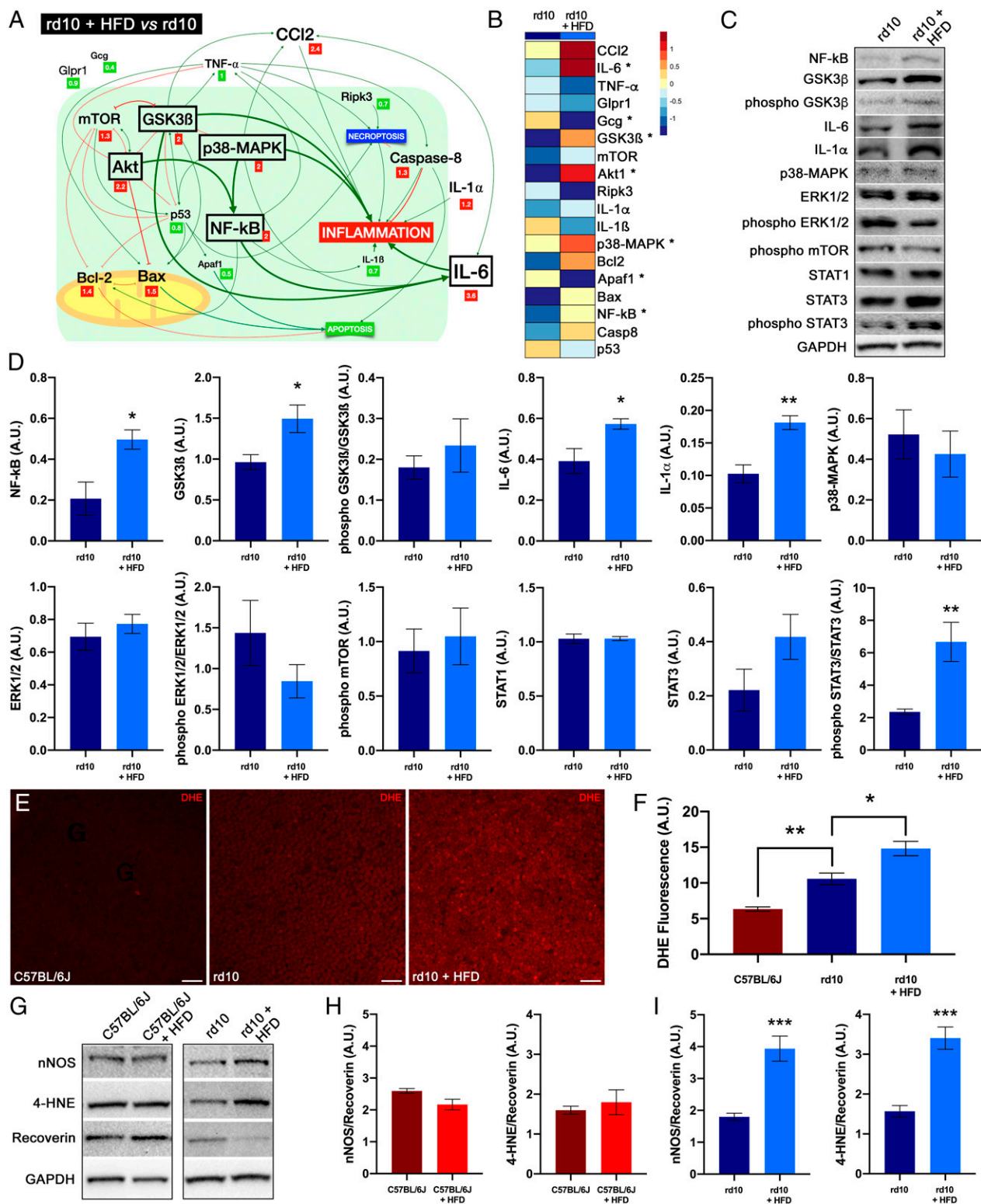
Short-Term HFD Modulates Inflammation- and Cell Death–Related Pathways in RP Mice.

To evaluate the effects of short-term HFD on inflammation and cell death, we analyzed the expression levels of some key genes in the retinas of normal and rd10 mice on HFD or chow for 2 wk. We found significantly higher levels of CCl2 (4.8-fold), IL-6 (2.2-fold), TNF-α (2.0-fold), Ripk3 (2.1-fold), and caspase 8 (2.5-fold) in the retinas of chow-fed rd10 mice compared with control mice on the same diet (*SI Appendix*, Table S3). HFD consumption caused minor changes in the expression of genes related to inflammation and cell death in control mice (*SI Appendix*, Fig. S2 and Table S4). By contrast, in rd10 mice, short-term HFD increased the messenger RNA (mRNA) levels of IL-6 (3.6-fold), Akt1 (2.2-fold), GSK3β (2.0-fold), p38-MAPK (2.0-fold), and NF-κB (2.1-fold) as compared with chow diet (Fig. 5 *A* and *B* and *SI Appendix*, Table S5). Moreover, the retinas of rd10 mice on an HFD showed a nonsignificant increase in the expression of CCl2 (2.4-fold) with respect to chow-fed rd10 mice. The increase in mRNA levels of CCl2, IL-6, and NF-κB on the HFD pointed to an exacerbation of inflammation in rd10 mice. HFD also induced a significant decrease in Gcg and Apaf1 expression levels in the retinas of rd10 mice (0.4- and 0.5-fold, respectively). Western blotting confirmed the increased expression of GSK3β, NF-κB, and IL-6 in HFD-fed rd10 mice and revealed augmented levels of phospho-STAT3/STAT3 and IL-1α (Fig. 5 *C* and *D*), supporting the triggering effect of HFD on the GSK3β and NF-κB/IL-6/STAT3 signaling pathways. No significant changes were observed in ERK1/2, p38-MAPK, STAT1, or

STAT3 nor in the phosphorylated forms of GSK3β, ERK1/2, and mTOR levels in HFD-fed rd10 mice (Fig. 5 *C* and *D*), and no significant increases in inflammatory modulators were observed in HFD-fed control mice (*SI Appendix*, Fig. S2).

Short-Term HFD Exposure Enhances Oxidative Stress in RP Mice.

To assess intracellular oxidative stress in photoreceptor cells, we used dihydroethidium (DHE), a cell membrane–permeable fluorescent probe used for determining the sites of superoxide anion formation. Whole-mount retinas from control animals revealed only a few DHE-labeled cells (Fig. 5*E*), independently of the diet consumed. By contrast, rd10 mice showed higher DHE staining at the photoreceptor layer (Fig. 5*E*), and fluorescence intensity was stronger in the retinas from HFD-fed animals than from chow-fed counterparts (Fig. 5*F*). Western blot analysis revealed higher levels of neuronal nitric oxide synthase (nNOS), a marker of reactive nitrogen species, and 4-hydroxynonenal (4-HNE), a product of lipid peroxidation, in retinas from HFD-fed rd10 mice (Fig. 5 *G–I*). No significant changes in nNOS and 4-HNE abundance were observed in control mice on HFD. In all measures, nNOS and 4-HNE levels were normalized to those of recoverin, proportional to the density of photoreceptors. These results point to a pro-oxidative effect of high-diet consumption in the retina of RP mice.
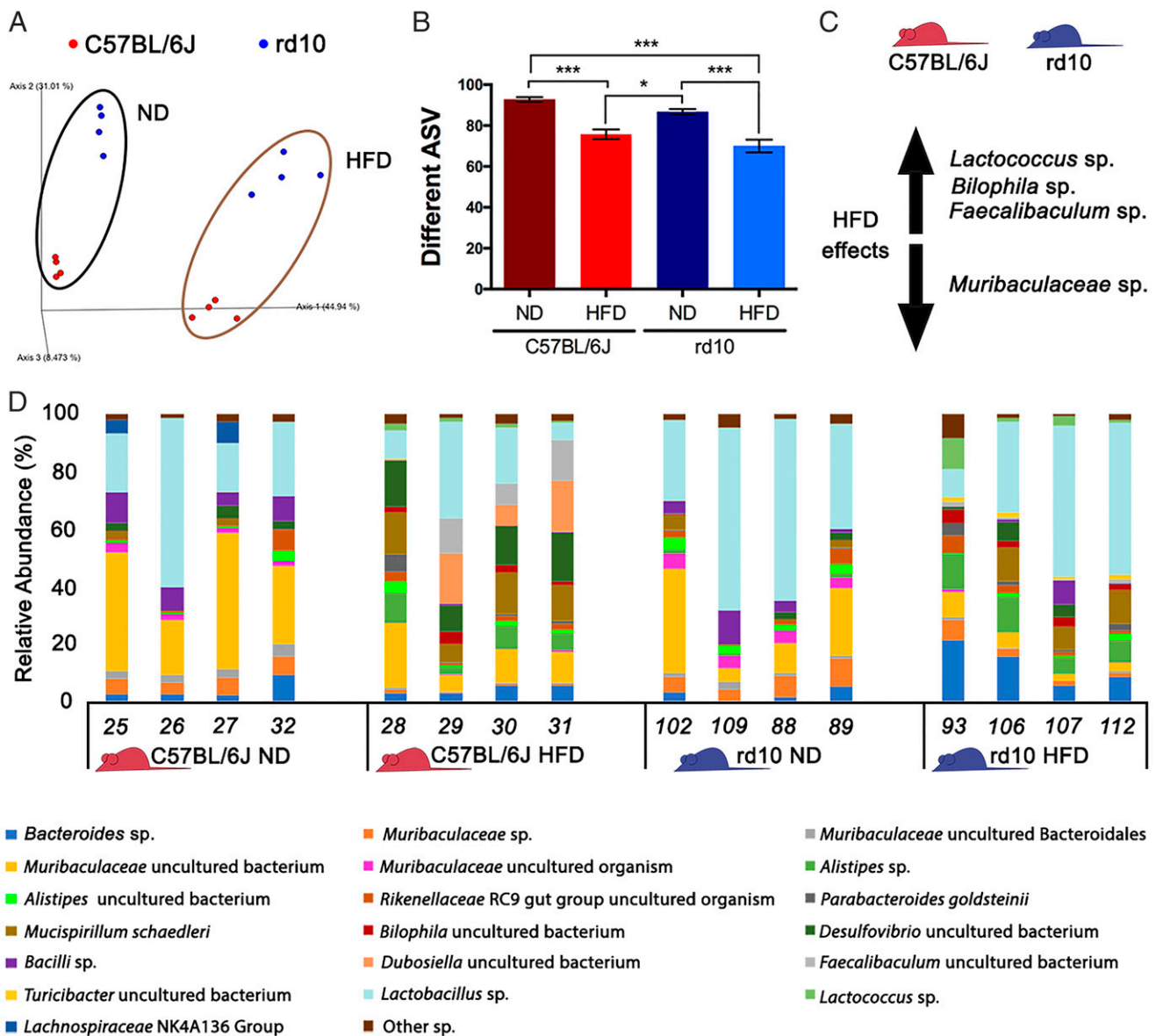
HFD Consumption Alters the Gut Microbiome.

To explore the effect of HFD feeding on the gut microbiota, we extracted DNA from the gut tissue and stool of mice on the different diets and used 16S ribosomal RNA (rRNA) gene amplification/sequencing on the Illumina platform to survey the microbiome. The sequenced data were processed using QIIME2. Differences in microbiome beta diversity were observed between the HFD and chow diet groups in both control and rd10 mice (unweighted UniFrac, weighted UniFrac, Bray–Curtis and Jaccard; *SI Appendix*, Table S6 and Fig. 6*A*). Differences were also observed between rd10 and control mice with all distance metrics tested (*SI Appendix*, Table S6) with the exception of the weighted UniFrac distance, which considers the relative bacterial abundance. Regarding alpha diversity, the richness of the total number of bacterial genera and amplicon sequence variant abundance (Fig. 6*B*) was higher for mice fed chow diet, and these differences were significant when data were analyzed considering both diet (chow versus HFD) and mouse genotype (rd10 versus C57BL/6J) as factors (*SI Appendix*, Table S7). Diet also produced a significant difference in the Faith diversity index (FDI control diet > FDI HFD) because of phylogenetic changes, as evenness was not significant (Pielou's Evenness, Shannon's Index; *SI Appendix*, Table S7).

Regarding taxonomy, principal coordinate analyses collapsed at different taxa levels, showing that the diet influenced the microbiome from family to species level (*SI Appendix*, Fig. S3). At the species level, 19 were abundant (>1% of relative abundance) and common in all samples with a variable average of cumulative relative abundance (49.33 to 68.00%) depending on the sample (Fig. 6*D*). Variations were further explored with the analysis of comparisons on microbiome (ANCOM) test, which revealed significant differences at the species level in the abundance of *Lactococcus* sp. (W = 45), *Bilophila* sp. (W = 37), and *Faecalibaculum* sp. (W = 42), which were favored in mice fed HFD. By contrast, *Muribaculaceae* sp. (W = 34) was more abundant in mice on chow diet (Fig. 6*C*). The ANCOM results were confirmed with a permutual analysis of variance (PERMANOVA) or two-way ANOVA test followed by the post-hoc Tukey HSD (honestly significant differences) test, which showed that all *Muribaculaceae* spp. were more abundant in mice fed with the chow diet than with the HFD, whereas seven species were more abundant in HFD-fed mice (e.g., *Bacteroides*

Kutsyr et al.
Short-term high-fat feeding exacerbates degeneration in retinitis pigmentosa by promoting retinal oxidative stress and inflammation

PNAS | 7 of 12
https://doi.org/10.1073/pnas.2100566118

Fig. 5. Dietary fat affects cell mediators and oxidative stress. (*A*) Schematic view showing relative expression levels of cell mediators, their interactions, and their effects on inflammation in rd10 mice. Relative expression (fold change, in squares) of mRNAs in the retina was compared between mice fed a normal or HFD for 2 wk from postnatal day 19. The relative size of the letters represents the relative level of gene expression. Significant increases are marked by a box. (*B*) Heat map of the mean mRNA expression of cell mediators in rd10 mice fed normal chow or an HFD. Each grid element in the heat map is color-coded for the corresponding gene expression value. (*C* and *D*) Detection of cell mediators by Western blotting in the retina of rd10 mice fed HFD or normal chow. GAPDH levels are shown as loading controls. (*E*) Whole-mount retinas showing the staining of DHE at the photoreceptor level in a C57BL/6J mouse fed normal chow and rd10 mice fed normal or an HFD. (*F*) Quantification of DHE fluorescence. (*G–I*) Detection of nNOS (*H*) and 4-HNE (*I*) by Western blotting (*G*) in the retina of rd10 mice fed an HFD or normal chow. GAPDH levels are shown as loading controls. ANOVA, Bonferroni's test, diet effects (normal versus HFD) on mRNA levels, $n = 4$, *$P < 0.05$; Student's *t* test, diet effects (normal versus HFD) on protein levels, $n = 4$ to 7, *$P < 0.05$, **$P < 0.01$, ***$P < 0.001$; Kruskal–Wallis, Dunn's test, diet effects (normal versus HFD) on DHE fluorescence, $n = 3$ to 6, *$P < 0.05$, **$P < 0.01$. (Scale bars: 20 μm.)

Kutsyr et al.
Short-term high-fat feeding exacerbates degeneration in retinitis pigmentosa
by promoting retinal oxidative stress and inflammation

Fig. 6. Analysis of the mouse gut microbiome. (*A*) Unweighted UniFrac distance represented as a principal coordinate analysis for rd10 (in blue) and C57BL/6J mice (in red) where the influence of the diet could be observed (ND: normal diet). (*B*) Richness analysis comparing the number of amplicon sequence variants (ASVs) for C57BL/6J (red bars) or rd10 (blue bars) mice fed a ND or HFD. (*C*) Main effects of an HFD on the microbiome of the studied mice (C57BL/6J and rd10) regarding species abundance variation according to the ANCOM test. Increase is indicated by the arrow pointing up (*Lactococcus* sp., *Bilophila* sp., and *Faecalibaculum* sp.), whereas decrease is indicated by the arrow pointing down (*Muribaculaceae* sp.). (*D*) Relative abundance (%) of gut microbiome species that showed more than 1% of relative abundance in one sample. Bar plot was performed for C57BL/6J (in red) or rd10 mice (in blue) fed ND or HFD. ANOVA, Tukey HSD test, diet and mouse strain effect, $n = 4$, *$P < 0.05$, ***$P < 0.001$.

sp., *Parabacteroides goldsteinii*, *Alistipes* sp., and *Mucispirillum schaedleri*; *SI Appendix*, Table S8).

Discussion

The effects of dietary fat on retinal function and structure have garnered considerable interest in recent years. In the present study, we demonstrate that a short-term increase in dietary fat intake aggravates retinal degeneration in a mouse model of RP. Increased dietary fat intake reduces retinal responsiveness and photoreceptor cell number in dystrophic rd10 mice, which is accompanied by the deterioration of photoreceptor morphology and synaptic contacts at the OPL. These findings are in line with previous studies showing that fat intake positively associates with

a risk of age-related macular degeneration (19) and that retinal cell dysfunction is enhanced by short-term increases in dietary fat and sucrose (28). Similar effects have been described in the brain, in which it has been shown that HFD exacerbates the progression of Parkinson's disease (29), Alzheimer's disease (30), and other forms of cognitive impairment (31). Arguing against this, however, are the findings of neuroprotective effects of low-protein, high-fat ketogenic diets in rd10 mice (20) and after *N*-methyl-D-aspartate (NMDA)-induced damage in the rat retina (32). The differences between our study findings and those of the aforementioned studies might relate to the macronutrient proportions of the diet and to the possible neuroprotective effects of ketone bodies (20). It must also be considered that the effects of dietary fat on retinal degeneration might depend on

Kutsyr et al.
Short-term high-fat feeding exacerbates degeneration in retinitis pigmentosa by promoting retinal oxidative stress and inflammation

PNAS | 9 of 12
https://doi.org/10.1073/pnas.2100566118

the fat composition. For example, a higher intake of mono- and polyunsaturated fatty acids is associated with a decreased risk for age-related macular degeneration (33). Our findings confirm that dietary fat influences degenerative processes in retinal neurodegenerative diseases, but the relative contribution and importance of individual dietary components remain unknown. Nonetheless, the role of HFD in determining neuronal susceptibility to damage is relevant to patients with retinal degeneration, who should limit their daily fat intake.

HFD feeding for 2 or 3 wk increased body weight, glycemia, and glucose intolerance in both wild-type (control) and RP (rd10) mice, confirming other studies showing that acute HFD feeding disrupts glucose homeostasis in both healthy mice (4) and in humans (34) by increasing plasma glucose and insulin and impairing glucose tolerance and insulin sensitivity (34). Interestingly, we found that the HFD-induced changes in glucose homeostasis were reversed by cessation of the HFD for 2 wk, which aligns with previous work demonstrating that a 2-wk low-fat diet restores metabolic parameters after a 5-wk high-fat feeding regimen (35). Our results also show that HFD-induced impairment of glucose tolerance is more severe in RP mice. This suggests that retinal neurodegenerative disease affects not only retinal homeostasis but also involves alterations in the endocrine and metabolic response to feeding, possibly through changes in the systemic inflammatory state, oxidative stress, or other processes. Inflammatory findings associated with photoreceptor degeneration in various retinal degeneration diseases have been observed in both animal models and humans (36), and likewise, an altered antioxidant–oxidant status has been reported in the peripheral blood of patients with RP (37).
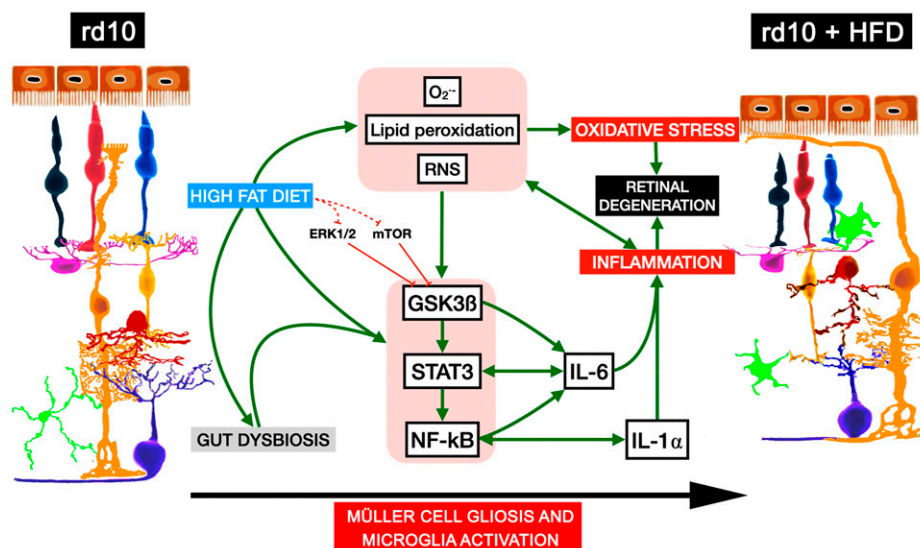
In good agreement with previous data (6), our study reveals that HFD triggers marked gut microbiome dysbiosis, affecting both the alpha and beta diversity of the gut bacteria. In a previous study, we found differences between normal chow-fed rd10 and C57BL6/J mice in inflammation-related bacterial species, which have been associated with neurodegenerative diseases (38). Here, we found that HFD increased the abundance of *Bilophila* sp (39), *Alistipes* sp., and *Mucispirillum schaedleri* (40), which have been previously described to correlate positively with gut inflammation processes in mice subjected to HFD (41). HFD-fed mice also showed a significant decrease of commensal bacteria such as *Muribaculaceae*, which are related to gut homeostasis (42). While the molecular and cellular mechanisms that underlie HFD-induced neurodegeneration remain poorly understood, it has been previously reported that HFD induces acute and chronic neuroinflammation (43), neurodegeneration, and cognitive impairment (44, 45). Accordingly, one possibility is that high-fat feeding drives retinal neuroinflammation through the induction of reactive gliosis and through increases in microglial density (46, 47). Consistent with this, we found that HFD feeding in RP mice specifically augments the activation of retinal microglia and macroglia, which accords with a study showing that lipopolysaccharide-induced systemic inflammation accelerates retinal neurodegeneration in dystrophic P23H rats (24), an animal model of RP, without inducing significant functional or morphological changes in the retina of healthy rats. Comparable results were reported in a prior study in which HFD feeding potentiated the expression of proinflammatory cytokines in the brain of only those animals peripherally challenged with lipopolysaccharide (48). Thus, the gut dysbiosis caused by HFD might promote retinal inflammatory processes, which, in turn, might accelerate retinal degeneration in rd10 mice as described for other neurodegenerative diseases (10, 11). In support of this hypothesis, HFD-induced gut dysbiosis has been reported to trigger intestinal inflammation and increase the levels of proinflammatory cytokines that influence retinal degeneration (49). Likewise, it has been demonstrated that retinal impairment caused by HFD involves

activation of inflammatory signaling pathways through a mechanism mediated by TLR4 (12).

Molecular analysis indicated that HFD induces the up-regulation of the GSK3β and NF-κB/IL-6/STAT3 signaling pathways in rd10 mice. GSK3β is a key protein in the inflammatory response (50), and its activation has been related to retinal degeneration and the accompanying inflammation in animal models of RP (24). Indeed, inhibitors of GSK3β have been proposed for the treatment of RP (51). STAT3 is a known transcription factor for GFAP in Müller glia directly related to gliosis, a common process in many neurodegenerative diseases of the retina including RP (52). A central role for STAT signaling has been reported in the rd10 mouse model of RP (53). In the same line, NF-κB is a key regulator of inflammation (54) and has been proposed to have a neurotoxic role in rd10 mice during photoreceptor degeneration by activating microglia (55). Retinal NF-κB expression is increased in different injury models such as those induced by light (56) or ischemia (57). More recently, it has been demonstrated that HFD up-regulates the expression NF-κB in retinal cells (58). Thus, the enhanced expression of GSK3β in the retina of HFD-fed rd10 mice together with the increased levels of phospho-STAT3 and NF-κB indicate that the high-fat feeding effects on retinal degeneration are likely due to activation of the GSK3β/STAT3/NF-κB signaling pathway, leading to elevated levels of IL-6 and IL-1α, which play a main role in ocular inflammatory diseases (59, 60). This evidence is reinforced by the down-regulation of key proteins of alternative signaling pathways as the transcription factor STAT1 and p38-MAPK and ERK1/2 kinases. While short-term HFD induced a robust immune response in the retina of rd10 mice, our results suggest that neither necroptosis nor apoptosis cell death pathways are activated, as HFD failed to modify the mRNA expression levels of Ripk3, p53, Bax, and Bcl-2 and significantly reduced Apaf1 expression.

Oxidative stress is another possible contributor to the HFD-induced neurodegenerative changes in rd10 mice. Reactive oxygen species (ROS) can be generated in high amounts in the retina due to the high concentrations of oxygen, an abundance of polyunsaturated fatty acids, and direct exposure to light (61). Moreover, ROS can induce the production of several proinflammatory cytokines (including IL-6), activate NF-κB, and trigger the activation of the inflammasome (62). In this context, a previous analysis has shown that HFD feeding is associated with elevated neuronal oxidative stress and blunted antioxidant responses (63). We found that rd10 mice fed an HFD had a relatively higher production of superoxide at the photoreceptor layer than equivalent mice on normal chow, and this was accompanied by higher levels of both nNOS, which is involved in the production of reactive nitrogen species, and 4-HNE, an indicator of lipid peroxidation. These findings agree with previous work showing that HFD feeding in mice results in higher levels of inducible NOS and 4-hydroxynonenal and with retinal degeneration (64). It should also be noted that nonsignificant changes in oxidative stress were observed in HFD-fed control mice. It is possible that the HFD-induced effects on cellular redox balance are compensated for in healthy animals by antioxidant mechanisms (65), whereas the breakdown of this redox balance by disease may lead to exacerbated ROS production.

In summary, our findings establish that short-term HFD consumption in mice with RP induces significant alterations in retinal function and structure through mechanisms that may involve changes in the gut microbiome, the retinal inflammatory state, and retinal redox homeostasis (Fig. 7). We propose that HFD consumption and the subsequent gut microbiota dysbiosis trigger the expression and production of the inflammatory modulators GSK3β, STAT3, and NF-κB in mice with RP, which in turn enhances the expression and release of the proinflammatory cytokines IL-6 and IL-1α by activated microglia

Kutsyr et al.
Short-term high-fat feeding exacerbates degeneration in retinitis pigmentosa by promoting retinal oxidative stress and inflammation

Fig. 7. Proposed mechanisms for high-fat diet-induced retinal degeneration in RP mice. HFD consumption and gut microbiota dysbiosis in rd10 mice induce increased expression and activity of the inflammatory modulators GSK3β, STAT3, and NF-κB and the expression and release of the inflammatory cytokines IL-6 and IL-1α. HFD feeding also promotes production and accumulation of reactive oxygen and nitrogen species and lipid peroxidation, causing redox imbalance and greater induction of the inflammatory response. Inflammation and oxidative stress lead to acceleration of the degenerative process and retinal remodeling. $O_2^{\cdot-}$: superoxide anion, RNS: reactive nitrogen species.

and Müller cells, without the involvement of ERK1/2 and mTOR. In parallel, HFD feeding promotes the production and accumulation of ROS and reactive nitrogen species and the oxidation of lipids, overall causing redox imbalance and inducing the inflammatory cascade. This scenario of inflammation and oxidative stress exacerbates the degenerative process and retinal remodeling (Fig. 7). The results can be extrapolated to other retinal diseases associated with inflammation and oxidative stress, such as glaucoma or macular degeneration. Our findings suggest that dietary fat intake affects the progression of disease in patients with ocular degenerative disorders and that it would be recommendable for these patients to increase their knowledge and awareness of appropriate dietary fat consumption.

Materials and Methods

Rd10 and C57BL/6J mice were fed for 2 or 3 wk from postnatal day 19 with normal chow (5.5% fat kcal) or with an HFD (61.6% fat kcal). The animals were weighed, and blood glucose levels were determined after the dietary periods. Retinal function was assessed by the optomotor test and electroretinography. The morphological integrity of the retinas was evaluated by staining retina cross-sections with hematoxylin or by immunohistochemistry. The retinal expression of inflammatory and cell death markers was analyzed by qRT-PCR and Western blotting. The oxidative state of the retinas was evaluated using a redox-sensitive probe and Western blotting. Gut microbiome from the gut tissue and stool (the cecum and its contents) was analyzed by 16S rRNA gene sequencing. For details on the methods used, please refer to *SI Appendix, SI Materials and Methods*. Current guidelines and regulations for the use of laboratory animals (NIH, Association for Research in Vision and Ophthalmology, and European Directive 2010/63/EU) were applied to maintain and handle the animals and comply with the Reporting of In Vivo Experiments guidelines of animal research in an effort to minimize their suffering and limit the number of animals used. The approval for all procedures was obtained from the ethics committee for animal care and use at the University of Alicante (UA-2018-07-06).

Data Availability. All study data are included in the article and/or *SI Appendix*.

1. D. Yach, D. Stuckler, K. D. Brownell, Epidemiologic and economic consequences of the global epidemics of obesity and diabetes. *Nat. Med.* **12**, 62–66 (2006).

2. B. Reynés, M. Palou, A. Palou, Gene expression modulation of lipid and central energetic metabolism related genes by high-fat diet intake in the main homeostatic tissues. *Food Funct.* **8**, 629–650 (2017).

3. R. S. Surwit, C. M. Kuhn, C. Cochrane, J. A. McCubbin, M. N. Feinglos, Diet-induced type II diabetes in C57BL/6J mice. *Diabetes* **37**, 1163–1167 (1988).

4. M. S. Wiedemann, S. Wueest, F. Item, E. J. Schoenle, D. Konrad, Adipose tissue inflammation contributes to short-term high-fat diet-induced hepatic insulin resistance. *Am. J. Physiol. Endocrinol. Metab.* **305**, E388–E395 (2013).

5. Y. Ji et al., Short term high fat diet challenge promotes alternative macrophage polarization in adipose tissue via natural killer T cells and interleukin-4. *J. Biol. Chem.* **287**, 24378–24386 (2012).

6. E. A. Murphy, K. T. Velazquez, K. M. Herbert, Influence of high-fat diet on gut microbiota: A driving force for chronic disease risk. *Curr. Opin. Clin. Nutr. Metab. Care* **18**, 515–520 (2015).

7. M. W. Rohr, C. A. Narasimhulu, T. A. Rudeski-Rohr, S. Parthasarathy, Negative effects of a high-fat diet on intestinal permeability: A review. *Adv. Nutr.* **11**, 77–91 (2020).

8. J. M. Duarte, Metabolic alterations associated to brain dysfunction in diabetes. *Aging Dis.* **6**, 304–321 (2015).

9. V. Frisardi et al., Metabolic-cognitive syndrome: A cross-talk between metabolic syndrome and Alzheimer's disease. *Ageing Res. Rev.* **9**, 399–417 (2010).

10. S. K. Sah, C. Lee, J. H. Jang, G. H. Park, Effect of high-fat diet on cognitive impairment in triple-transgenic mice model of Alzheimer's disease. *Biochem. Biophys. Res. Commun.* **493**, 731–736 (2017).

11. J. K. Morris, G. L. Bomhoff, J. A. Stanford, P. C. Geiger, Neurodegeneration in an animal model of Parkinson's disease is exacerbated by a high-fat diet. *Am. J. Physiol. Regul. Integr. Comp. Physiol.* **299**, R1082–R1090 (2010).

12. J. J. Lee et al., High-fat diet induces toll-like receptor 4-dependent macrophage/microglial cell activation and retinal impairment. *Invest. Ophthalmol. Vis. Sci.* **56**, 3041–3050 (2015).

13. R. C. A. Chang et al., High-fat diet-induced retinal dysfunction. *Invest. Ophthalmol. Vis. Sci.* **56**, 2367–2380 (2015).

14. M. Coucha et al., High fat diet dysregulates microRNA-17-5p and triggers retinal inflammation: Role of endoplasmic-reticulum-stress. *World J. Diabetes* **8**, 56–65 (2017).

Kutsyr et al.
Short-term high-fat feeding exacerbates degeneration in retinitis pigmentosa
by promoting retinal oxidative stress and inflammation

PNAS | **11 of 12**
https://doi.org/10.1073/pnas.2100566118

15. I. N. Mohamed *et al.*, Thioredoxin-interacting protein is required for endothelial NLRP3 inflammasome activation and cell death in a rat model of high-fat diet. *Diabetologia* **57**, 413–423 (2014).

16. L. Gao *et al.*, High prevalence of diabetic retinopathy in diabetic patients concomitant with metabolic syndrome. *PLoS One* **11**, e0145293 (2016).

17. H. Ghaem Maralani *et al.*, Metabolic syndrome and risk of age-related macular degeneration. *Retina* **35**, 459–466 (2015).

18. E. Rinninella *et al.*, The role of diet, micronutrients and the gut microbiota in age-related macular degeneration: New perspectives from the gut–retina axis. *Nutrients* **10**, 1677 (2018).

19. E. W. T. Chong *et al.*, Fat consumption and its association with age-related macular degeneration. *Arch. Ophthalmol.* **127**, 674–680 (2009).

20. R. C. Ryals *et al.*, A ketogenic & low-protein diet slows retinal degeneration in rd10 mice. *Transl. Vis. Sci. Technol.* **9**, 18 (2020).

21. A. Noailles *et al.*, The absence of toll-like receptor 4 mildly affects the structure and function in the adult mouse retina. *Front. Cell. Neurosci.* **13**, 59 (2019).

22. L. Campello *et al.*, New Nrf2-inducer compound ITH12674 slows the progression of retinitis pigmentosa in the mouse model rd10. *Cell. Physiol. Biochem.* **54**, 142–159 (2020).

23. P. Lax, G. Esquiva, C. Altavilla, N. Cuenca, Neuroprotective effects of the cannabinoid agonist HU210 on retinal degeneration. *Exp. Eye Res.* **120**, 175–185 (2014).

24. A. Noailles, V. Maneu, L. Campello, P. Lax, N. Cuenca, Systemic inflammation induced by lipopolysaccharide aggravates inherited retinal dystrophy. *Cell Death Dis.* **9**, 350 (2018).

25. L. Fernández-Sánchez *et al.*, Controlled delivery of tauroursodeoxycholic acid from biodegradable microspheres slows retinal degeneration and vision loss in P23H rats. *PLoS One* **12**, e0177998 (2017).

26. A. Noailles *et al.*, Persistent inflammatory state after photoreceptor loss in an animal model of retinal degeneration. *Sci. Rep.* **6**, 33356 (2016).

27. O. Kutsyr *et al.*, Gradual increase in environmental light intensity induces oxidative stress and inflammation and accelerates retinal neurodegeneration. *Invest. Ophthalmol. Vis. Sci.* **61**, 1 (2020).

28. V. Chrysostomou, P. van Wijngaarden, G. R. Steinberg, J. G. Crowston, A short term high-fat high-sucrose diet in mice impairs optic nerve recovery after injury and this is not reversed by exercise. *Exp. Eye Res.* **162**, 104–109 (2017).

29. M. Bousquet *et al.*, High-fat diet exacerbates MPTP-induced dopaminergic degeneration in mice. *Neurobiol. Dis.* **45**, 529–538 (2012).

30. P. Thériault, A. ElAli, S. Rivest, High fat diet exacerbates Alzheimer's disease-related pathology in APPswe/PS1 mice. *Oncotarget* **7**, 67808–67827 (2016).

31. Z. A. Cordner, K. L. K. Tamashiro, Effects of high-fat diet exposure on learning & memory. *Physiol. Behav.* **152**, 363–371 (2015).

32. T. Zarnowski *et al.*, Ketogenic diet attenuates NMDA-induced damage to rat's retinal ganglion cells in an age-dependent manner. *Ophthalmic Res.* **53**, 162–167 (2015).

33. M. Roh *et al.*, Higher intake of polyunsaturated fatty acid and monounsaturated fatty acid is inversely associated with AMD. *Invest. Ophthalmol. Vis. Sci.* **61**, 20 (2020).

34. L. K. Heilbronn, L. V. Campbell, A. Xu, D. Samocha-Bonet, Metabolically protective cytokines adiponectin and fibroblast growth factor-21 are increased by acute overfeeding in healthy humans. *PLoS One* **8**, e78864 (2013).

35. Y. Shang *et al.*, Short term high fat diet induces obesity-enhancing changes in mouse gut microbiota that are partially reversed by cessation of the high fat diet. *Lipids* **52**, 499–511 (2017).

36. J. J. McMurtrey, M. O. M. Tso, A review of the immunologic findings observed in retinitis pigmentosa. *Surv. Ophthalmol.* **63**, 769–781 (2018).

37. C. Martínez-Fernández de la Cámara *et al.*, Altered antioxidant-oxidant status in the aqueous humor and peripheral blood of patients with retinitis pigmentosa. *PLoS One* **8**, e74223 (2013).

38. O. Kutsyr *et al.*, Retinitis pigmentosa is associated with shifts in the gut microbiome. *Sci. Rep.* **11**, 6692 (2021).

39. J. M. Natividad *et al.*, Bilophila wadsworthia aggravates high fat diet induced metabolic dysfunctions in mice. *Nat. Commun.* **9**, 2802 (2018).

40. A. Loy *et al.*, Lifestyle and horizontal gene transfer-mediated evolution of *Mucispirillum schaedleri*, a core member of the murine gut microbiota. *mSystems* **2**, e00171-16 (2017).

41. L. Arias *et al.*, Influence of gut microbiota on progression to tuberculosis generated by high fat diet-induced obesity in C3HeB/FeJ mice. *Front. Immunol.* **10**, 2464 (2019).

42. J. K. Volk *et al.*, The Nlrp6 inflammasome is not required for baseline colonic inner mucus layer formation or function. *J. Exp. Med.* **216**, 2602–2618 (2019).

43. P. S. Dalvi *et al.*, High fat induces acute and chronic inflammation in the hypothalamus: Effect of high-fat diet, palmitate and TNF-α on appetite-regulating NPY neurons. *Int. J. Obes.* **41**, 149–158 (2017).

44. C. M. Duffy, J. J. Hofmeister, J. P. Nixon, T. A. Butterick, High fat diet increases cognitive decline and neuroinflammation in a model of orexin loss. *Neurobiol. Learn. Mem.* **157**, 41–47 (2019).

45. P. J. Pistell *et al.*, Cognitive impairment following high fat diet consumption is associated with brain inflammation. *J. Neuroimmunol.* **219**, 25–32 (2010).

46. I. Hammoum *et al.*, Study of retinal alterations in a high fat diet-induced type ii diabetes rodent: *Meriones shawi*. *Acta Histochem.* **119**, 1–9 (2017).

47. D. A. Clarkson-Townsend *et al.*, Impacts of high fat diet on ocular outcomes in rodent models of visual disease. *Exp. Eye Res.* **204**, 108440 (2021).

48. C. Boitard *et al.*, Impairment of hippocampal-dependent memory induced by juvenile high-fat diet intake is associated with enhanced hippocampal inflammation in rats. *Brain Behav. Immun.* **40**, 9–17 (2014).

49. E. M. Andriessen *et al.*, Gut microbiota influences pathological angiogenesis in obesity-driven choroidal neovascularization. *EMBO Mol. Med.* **8**, 1366–1379 (2016).

50. L. Hoffmeister, M. Diekmann, K. Brand, R. Huber, GSK3: A kinase balancing promotion and resolution of inflammation. *Cells* **9**, 820 (2020).

51. M. Marchena *et al.*, Small molecules targeting glycogen synthase kinase 3 as potential drug candidates for the treatment of retinitis pigmentosa. *J. Enzyme Inhib. Med. Chem.* **32**, 522–526 (2017).

52. S. L. Roche, A. M. Ruiz-Lopez, J. N. Moloney, A. M. Byrne, T. G. Cotter, Microglial-induced Müller cell gliosis is attenuated by progesterone in a mouse model of retinitis pigmentosa. *Glia* **66**, 295–310 (2018).

53. A. Ly *et al.*, Proteomic profiling suggests central role Of STAT signaling during retinal degeneration in the rd10 mouse model. *J. Proteome Res.* **15**, 1350–1359 (2016).

54. T. Liu, L. Zhang, D. Joo, S. C. Sun, NF-κB signaling in inflammation. *Signal Transduct. Target. Ther.* **2**, 17023 (2017).

55. H. Y. Zeng, M. O. Tso, S. Lai, H. Lai, Activation of nuclear factor-kappaB during retinal degeneration in rd mice. *Mol. Vis.* **14**, 1075–1080 (2008).

56. T. Wu, Y. Chen, S. K. Chiang, M. O. Tso, NF-kappaB activation in light-induced retinal degeneration in a mouse model. *Invest. Ophthalmol. Vis. Sci.* **43**, 2834–2840 (2002).

57. Y. G. Chen, C. Zhang, S. K. Chiang, T. Wu, M. O. Tso, Increased nuclear factor-kappa B p65 immunoreactivity following retinal ischemia and reperfusion injury in mice. *J. Neurosci. Res.* **72**, 125–131 (2003).

58. X. Cao *et al.*, Effects of high-fat diet and Apoe deficiency on retinal structure and function in mice. *Sci. Rep.* **10**, 18601 (2020).

59. H. Ghasemi, Roles of IL-6 in ocular inflammation: A review. *Ocul. Immunol. Inflamm.* **26**, 37–50 (2018).

60. G. A. Kontadakis, A. Plaka, D. Fragou, G. D. Kymionis, A. M. Tsatsakis, *Chapter 19 - Ocular Biomarkers in Diseases and Toxicities,* R. C. Gupta, Ed. (Biomarkers in Toxicology, 2014), pp. 317–324.

61. M. Tuzcu *et al.*, Lutein and zeaxanthin isomers modulates lipid metabolism and the inflammatory state of retina in obesity-induced high-fat diet rodent model. *BMC Ophthalmol.* **17**, 129 (2017).

62. Y. Ruan, S. Jiang, A. Musayeva, A. Gericke, Oxidative stress and vascular dysfunction in the retina: Therapeutic strategies. *Antioxidants* **9**, 761 (2020).

63. B. L. Tan, M. E. Norhaizan, Effect of high-fat diets on oxidative stress, cellular inflammatory response and cognitive function. *Nutrients* **11**, 2579 (2019).

64. A. C. Marçal *et al.*, Diet-induced obesity impairs AKT signalling in the retina and causes retinal degeneration. *Cell Biochem. Funct.* **31**, 65–74 (2013).

65. Y. Nishimura, H. Hara, M. Kondo, S. Hong, T. Matsugi, Oxidative stress in retinal diseases. *Oxid. Med. Cell. Longev.* **2017**, 4076518 (2017).

12 of 12 | **PNAS**
https://doi.org/10.1073/pnas.2100566118

Kutsyr et al.
Short-term high-fat feeding exacerbates degeneration in retinitis pigmentosa by promoting retinal oxidative stress and inflammation